Proc. Natl. Acad. Sci. USA
Vol. 85, pp. 7988–7992, November 1988
Biophysics

Extracellular ATP induces a large nonselective conductance in macrophage plasma membranes

(extracellular tetra-anionic ATP/electrophysiology/K^+ conductances)

HENK P. BUISMAN*†‡, THOMAS H. STEINBERG§, JORGE FISCHBARG¶, SAMUEL C. SILVERSTEIN§, SAKE A. VOGELZANG*, CAN INCE*†‖, DIRK L. YPEY*, AND PETER C. J. LEIJH†

*Department of Physiology and Physiological Physics, University of Leiden, 2300 RC Leiden, The Netherlands; †Department of Infectious Diseases, University Hospital, 2333 AA Leiden, The Netherlands; §The Rover Laboratory of Physiology, Department of Physiology and Cellular Biophysics, and ¶Department of Ophthalmology, Columbia University College of Physicians and Surgeons, 630 West 168th Street, New York, NY

Communicated by Eric R. Kandel, June 8, 1988

ABSTRACT **Extracellular ATP in its tetra-anionic form (ATP^{4-}) induces ion fluxes and membrane depolarization in the mouse macrophage-like cell line J774.2 and in resident mouse macrophages. We analyzed the effects of extracellular ATP^{4-} by both patch-clamp and intracellular microelectrode techniques. Whole-cell patch-configuration membrane potential measurements on J774.2 cells revealed that ATP^{4-}-induced depolarization occurred within 40 ms of pulsed application of ATP and was completely reversible. The depolarizations were accompanied by a dramatic increase in membrane conductance and showed no sign of adaptation to ATP over a period of 30 min. At 5 mM total ATP (ATP_t) the whole-cell conductance was ≈10 nS, and an upper limit of 20 pS for a single-channel conductance has been established. The reversal potential associated with the ATP-induced depolarization at asymmetric K^+, Na^+, Ca^{2+}, and Cl^- concentrations across the membrane was 0 mV. In patch-clamped cells depolarization was complete at 20 μM ATP^{4-}, and repolarization from full depolarization occurred in ≈5 s. In contrast, in intact cells measured by microelectrode impalement, complete depolarization occurred at ≈2 mM ATP^{4-} and repolarization was much slower (≈100 min). These findings indicate that the changes in intracellular ionic composition that occur after ATP treatment affect the rate of cell repolarization. At lower concentrations of ATP, potassium conductances modulated the depolarizing effect of ATP. ATP also depolarized mouse peritoneal macrophages, but a variant cell line (ATPR B2), derived from J774.2 cells by prolonged exposure to ATP, was insensitive to ATP. Our results provide a membrane electrophysiological description and analysis of a large nonselective plasma membrane conductance of macrophages induced by extracellular ATP.**

Extracellular ATP permeabilizes the plasma membrane of mast cells (1) and murine macrophages (2, 3) to small membrane-impermeant molecules. ATP allows molecules as large as 831 D to enter the cytoplasmic matrix of mouse peritoneal macrophages and the mouse macrophage-like cell line J774.2 (4); incubation of these cells in medium containing ATP therefore rapidly collapses transmembrane electrochemical gradients (3). Permeabilization of J774.2 cells is induced by tetra-anionic ATP (ATP^{4-}) rather than $MgATP^{2-}$ and is inhibited or reversed by the addition of divalent cations. AMP-PNP, ATP[γS], and to a lesser degree ADP also permeabilize macrophages, but other nucleotide triphosphates are ineffective. By exposing J774.2 cells to ATP for prolonged durations, variant cell lines that are not permeabilized by extracellular ATP have been selected. Both the pharmacologic specificity of ATP permeabilization and the selection of ATP-resistant cell lines suggest that this phenomenon is mediated by ligation of a plasma membrane receptor for ATP^{4-}.

In this paper, we analyze the effects of extracellular ATP on the electrical properties of the plasma membrane of J774.2 cells and mouse peritoneal macrophages by patch-clamp and microelectrode techniques. ATP induced a large ion-nonselective conductance that was rapidly activated and fully reversible. This conductance may constitute a ligand-dependent channel with unusual properties.

MATERIALS AND METHODS

Cell Culture and Chemicals. The mouse macrophage cell line J774.2 (5) and an ATP-resistant variant (ATPR B2) derived from it (2) were grown in 50-ml tissue culture flasks in Dulbecco's modified Eagle's medium supplemented with 10% heat-inactivated (30 min, 56°C) fetal bovine serum/28 mM glucose/penicillin G (10^5 units per 100 ml of medium)/gentamicin (2 mg per 100 ml of medium). Cells were plated on 24-mm circular coverslips in 35-mm Petri dishes at a density of 10^5–10^6 cells per dish and were kept in culture for 0–5 days. Mouse peritoneal macrophages were harvested from male Swiss mice as described (6) and were cultured as described above. Na_2H_2ATP was purchased from Boehringer Mannheim. Concentrations of free ATP^{4-} were calculated as described by Fabiato and Fabiato (7).

Electrophysiology. Coverslips with adherent cells were mounted in a culture dish (8). The cells were bathed in an extracellular solution (ECS), consisting of 5.0 mM KCl/140 mM NaCl/1.0 mM $MgCl_2$/1.0 mM $CaCl_2$/10 mM Hepes/6.0 mM glucose, titrated with NaOH to pH 7.2. All experiments were performed at 26°C. ATP was either added to the bath or administered by means of a pressure ejection system (PPM-2 Medical Systems, Great Neck, NY). Ejection pipettes had apertures of 2–3 μm.

Conventional patch-clamp techniques were applied (9) in the cell-attached patch and whole-cell patch configurations with an EPC-5 patch-clamp amplifier (List Electronics, Darmstadt, F.R.G.). For whole-cell recordings, pipettes were filled with an intracellular-like solution of 140 mM KCl/10 mM NaCl/2.0 mM $MgCl_2$/1.0 mM $CaCl_2$/10 mM EGTA/10 mM Hepes titrated with KOH to pH 7.2. Patch pipettes had resistances of 3–7 MΩ.

Microelectrode impalement techniques were used to measure membrane potentials in intact cells. A rapid peak-shaped potential transient occurred within the first few milliseconds after penetration, as described for other mononuclear phago-

The publication costs of this article were defrayed in part by page charge payment. This article must therefore be hereby marked "*advertisement*" in accordance with 18 U.S.C. §1734 solely to indicate this fact.

Abbreviations: E_p, peak potential; ATP_t, total ATP.

‡To whom reprint requests should be addressed.
‖Present address: Department of Medical Physics, University of Amsterdam, 1105 AZ Amsterdam, The Netherlands.

cytes (10). The peak values of these transients (E_p, peak potential) were measured as indicators of the resting membrane potential existing before impalement (10). Microelectrodes were filled with 3 M KCl, had typical resistances of 50 MΩ (measured in 3 M KCl), and were compensated to time constants of <100 μs.

RESULTS

Membrane Depolarization Upon Pulsed Application of ATP. The whole-cell patch-clamp technique was applied to directly monitor membrane potential changes in individual cells upon ATP stimulation under conditions that maintained constant intra- and extracellular ionic concentrations. For this purpose, ATP pulses were applied by means of a pressure ejection system placed nearby the cell (Fig. 1). At zero time, ATP pulses of variable duration were applied. The membrane depolarized at an initial rate of ≈1 mV/ms. This rate indicates a lower limit of the depolarizing action of ATP, since it is limited by the properties of the ejection system and of the amplifier. The maximal depolarization for each record in Fig. 1 increased with pulse duration, indicating a dose dependency of the response to ATP (see also below, Fig. 4). Membrane potential at maximal depolarization approached 0 mV; for short pulses, depolarization occurred within 40 ms. Depolarization was sustained when pulse lengths were prolonged up to 10 s (data not shown), indicating that no desensitization of the receptor occurred on this time scale. Although the local ATP concentration in the vicinity of the cell may be slightly lower than the applied concentration of 4 mM, the delay in repolarization at the end of the longer pulses indicated that the local ATP concentration was supramaximal for fully depolarizing the cells. Cell repolarization upon terminating the ATP pulse was limited by the passive diffusion of ATP in the bath, since gently stirring the bath hastened this process (data not shown).

These experiments show that ATP depolarizes the macrophage membrane under controlled intracellular conditions, that ATP exerts its effects within milliseconds, that its effect is maintained and maximal as long as ATP is present at a sufficient concentration, and that the effect of ATP on membrane potential is fully reversible for brief application.

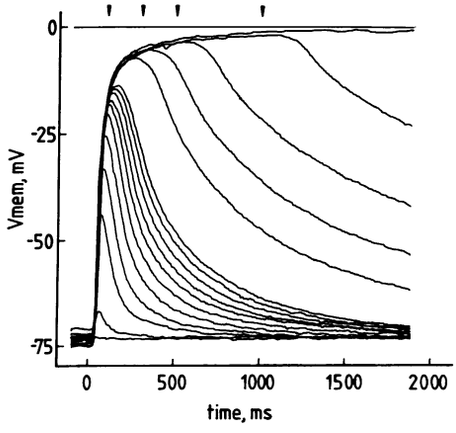

FIG. 1. Time courses of ATP-induced depolarizations of J774.2 cells upon pulsed application of ATP. The ejection pipette containing ECS with 4 mM ATP_t (1.9 mM ATP^{4-}) was placed within 6 μm of a cell in whole-cell patch configuration. Pulses of ATP were given with a pressure of 0.5 kg·cm^{-2} for 0, 10, 20, 30, 40, 50, 60, 70, 80, 90, 100, 200, 300, 500, 1000, and 2000 ms. Arrowheads indicate the end of the 200-, 300-, 500-, and 1000-ms pulses. Depolarization began after a short delay due to propagation of the pressure pulse through the ejection system. After termination of the pulses, membrane potentials (Vmem) completely recovered to the resting membrane potential (−75 mV). In control experiments, pulses of ECS alone did not affect the membrane potential (data not shown). Depolarization induced by pulsed application of ATP was observed in eight cells.

ATP^{4-} Rather than $MgATP^{2-}$ Depolarizes J774.2 Cells. Gomperts (11) and later Steinberg and Silverstein (2) showed that ATP^{4-} is the form of ATP that serves as a ligand for membrane permeabilization in mast cells and macrophages, respectively. To investigate whether the ATP-induced depolarizations under whole-cell patch conditions were induced by ATP^{4-}, membrane potentials and membrane resistances were measured in the whole-cell patch configuration while increasing [ATP^{4-}] by chelating divalent cations with EDTA. The cell shown in Fig. 2 had an initial membrane potential of −55 mV and a membrane resistance of ≈1 GΩ. Current pulses were injected to measure changes in membrane resistance. Application of 100 μM total ATP (ATP_t) to the bath resulted in a slight depolarization without a significant change in membrane resistance. Addition of EDTA induced a depolarization to 0 mV, while the membrane resistance decreased by a factor of ≈10. The slow rate of depolarization can be ascribed to the passive mixing of EDTA in the bath. Addition of EDTA alone induced transient fluctuations in membrane potential of ≈10 mV without significant change in membrane resistance (data not shown). These experiments indicate that ATP^{4-} is the membrane depolarizing agent and that partial as well as complete depolarization could be maintained for at least 5 min. Since ATP-hydrolyzing enzymes including the macrophage ectoprotein kinase (12) and the ectonucleoside triphosphatase (2) require Mg^{2+}, these experiments show directly that ATP hydrolysis is not required to activate this conductance and that kinases and nucleotidases are not involved in ATP-induced depolarization.

Properties of the ATP-Induced Conductance. To analyze the nature of the ATP-induced depolarization in more detail, the reversal potential of the ATP-induced pore was measured. For this purpose, ATP pulses were applied to cells in the whole-cell patch configuration while membrane potential transients were measured at different holding potentials, maintained by injecting different holding currents through the membrane. From all holding potentials, the membrane potential deflected toward 0 mV upon ATP stimulation (Fig. 3*A*). Maximal potential deflections are depicted as a function of holding membrane potentials in Fig. 3*B*. The reversal potential was 0 mV, which implies that the ATP-induced permeabilization is not selective for the various cations (Na^+, K^+, Ca^{2+}) in the solutions used.

To determine whether the ATP-induced pore was purely selective for Cl^-, we determined the reversal potential in cells bathed in an ECS in which >50% of the NaCl was replaced by sodium glutamate. This addition of glutamate and lowering of [Cl^-] did not change the resting membrane

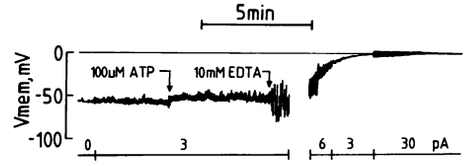

FIG. 2. Effect of subsequent addition of a low [ATP] and EDTA. Bath application of 100 μM ATP (4.6 μM ATP^{4-}) to a J774 cell in the whole-cell patch configuration induced a depolarization from −55 to −50 mV. Addition of 10 mM EDTA raised the concentration of ATP^{4-} to 87 μM and further depolarized the cell to 0 mV while the membrane resistance decreased by a factor of 10. The signal disturbances just before the blanked area are due to experimental manipulations. The peak to peak amplitude of the symmetric current injection pulses (duration, 500 ms; 1 Hz) used to measure the induced membrane resistance (Vmem) changes are indicated below the tracing. The magnitude of the membrane resistance can be estimated from the width of the tracing.

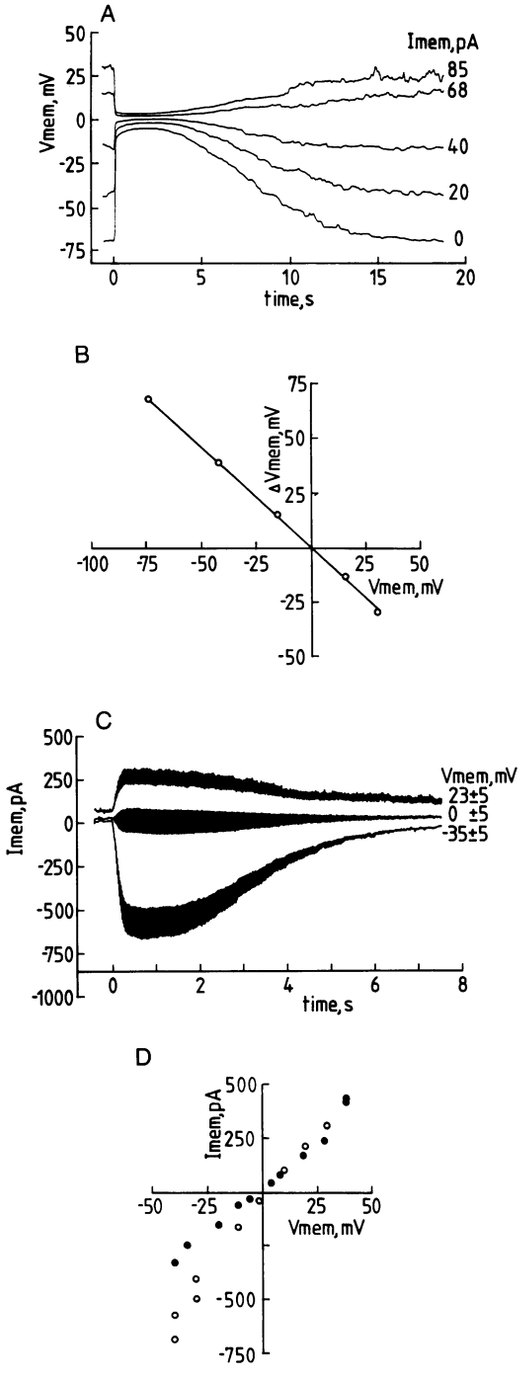

FIG. 3. Determination of the reversal potential of the ATP-induced pore in J774 cells in the whole-cell patch-clamp configuration. (*A*) Membrane potential transients upon 100-ms pulsed application of 5 mM ATP_t (2.7 mM ATP^{4-}). The holding membrane potential was varied by current injection (Imem). (*B*) Maximal amplitude of the membrane potential change (ΔVmem) as a function of holding potential (Vmem) obtained from the traces in *A*. The potential changes reverse polarity at 0 mV. (*C*) Current transients upon pulsed application of ATP (500 ms, same concentration as in *A*). Symmetric voltage pulses were given at various holding potentials as indicated. The size of the conductance can be estimated from the width of the trace and decreased as the concentration of ATP waned. (*D*) Maximal current of voltage-clamped cells upon pulsed application of ATP. The maximum of the current deflections of two cells are measured at various holding potentials. Maximal conductances are 7.7 and 14 nS. Slopes were estimated graphically from the linear part of the graph.

potential or slightly hyperpolarized it, indicating that glutamate does not have an excitatory action in J774.2 macrophages as it does in nerve cells. In the ECS of the ejection pipette, all NaCl was substituted by sodium glutamate to ensure asymmetric Cl^- concentrations across the membrane during ATP pulses. This asymmetry would shift the Nernst potential for Cl^- toward more positive values in instances of selective Cl^- permeability. However, in these experiments the average reversal potential was found to be −4.0 mV (four experiments; range, −13 to +1 mV), while the calculated values for the reversal potential for Cl^- were +18 to +54 mV.

From these experiments we conclude that the ATP-induced pore is selective neither for the cations in the solutions nor for the anions Cl^- and glutamate. This implies ion nonselectivity, consistent with previous findings (3, 4). To measure the amplitude of the ATP-activated conductance, ATP-induced current transients were measured at various stationary holding potentials under voltage-clamp conditions (Fig. 3*C*). The width of the tracings indicates the conductance changes that accompany the ATP-induced currents (see legend for details). The maximal values of these transients were plotted against the holding potentials in Fig. 3*D*, without correction for the background conductance. The maximal conductance induced by 5 mM ATP_t was ≈10 nS, a value that may be limited by the access resistance from the patch pipette to the cell. The ATP-induced conductance is linear around 0 mV and at positive potentials. The apparent rectification at hyperpolarizing potentials for one of the two cells may possibly be ascribed to inward rectifying conductances in the plasma membrane of this cell.

Is There a Unit Conductance? Single-channel events can be detected in current transients of fully inactivating conductances in voltage-clamped cells. In a similar fashion, we tried to detect single-channel events induced by ATP by applying pulses of ATP under voltage-clamp conditions. We analyzed the induced current transients (n = 3), paying special attention to the tails of the tracings, as the ATP effect waned. Although the transients were fully reversible, no quantal current steps were observed. We could therefore estimate an upper limit of 40 pS for a hypothetical ionic channel from the width of the current tracings (2 pA) and the applied driving forces (50 mV). We assumed that the channel openings were sufficiently large to be observed at the filter settings used (1 kHz; minimal detectable opening time, 0.5 ms). Even though all cells studied in the whole-cell patch configuration responded to ATP applied by the pressure pipette, only two out of four outside-out patches tested responded to ATP. From one of these outside-out patches, we could estimate an upper limit of 20 pS for a single-channel conductance by using the assumptions mentioned above. Furthermore, in cell-attached patch experiments, no single ionic channels were observed that could be ascribed to the action of extracellular ATP (n = 8) present in the pipette. Assuming that the channel openings were of sufficient duration to be observed at filter settings of 1 kHz, these cell-attached patch experiments would have allowed us to identify channels of a conductance as low as 10 pS if such channels had been present within the patched membrane.

Dose Dependency of ATP-Induced Depolarizations. In the whole-cell patch configuration, the intracellular ionic concentrations are "clamped" to those of the patch pipette. To determine the effect of ATP on the membrane potential of intact cells, where intracellular ionic concentrations can change in response to alterations in membrane permeability, we measured the effect of ATP on membrane potential by using microelectrode impalement. In the microelectrode impalement measurements (Fig. 4*A*), the $[ATP_t]$ in the bath was increased stepwise from 0 mM (control) until complete depolarization occurred (3.2 mM). The average membrane potential only gradually increased as the [ATP] increased. To check whether adaptive repolarization during incubation occurred, the cells were kept at 250 μM ATP_t for 30 min. At

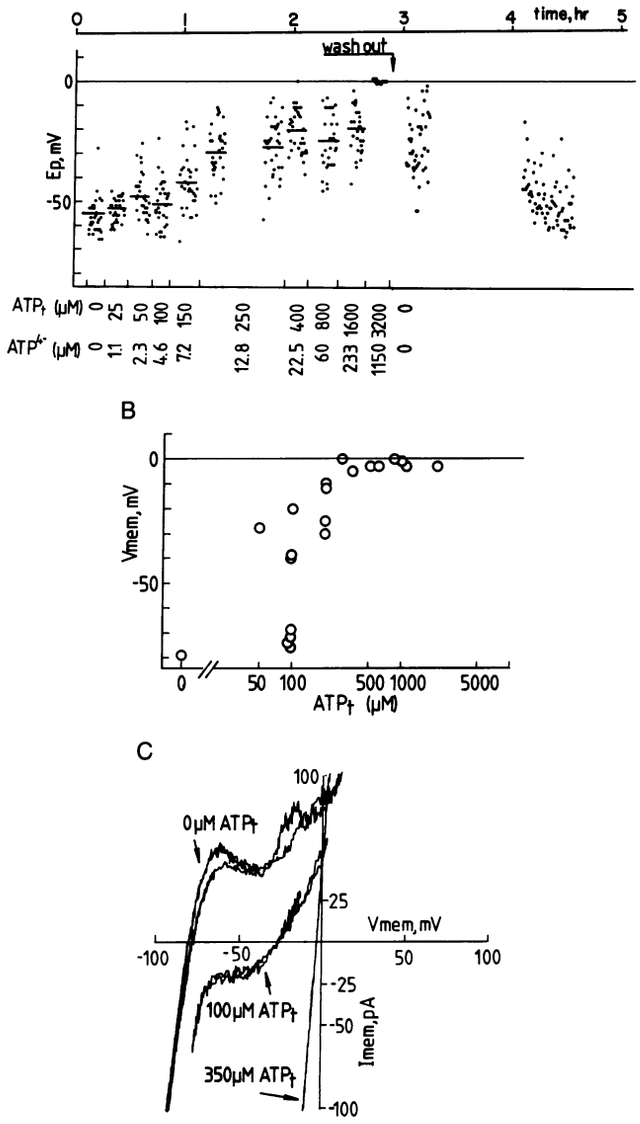

FIG. 4. Dependency of depolarization on ATP concentration. (*A*) Microelectrode impalement measurements showing individual E_p values in individual cells (·) as well as the mean values (—) of 30 impalements at each [ATP] applied. The calculated [ATP^{4-}] and [ATP_t] are indicated below the graph, and the time scale is indicated above the graph. After washout of ATP, the cells recovered from depolarization in ≈90 min. One of two experiments is shown. Each experiment was performed on one dish. (*B*) Membrane potentials (Vmem) of a cell in the whole-cell patch configuration at increasing and decreasing concentrations of ATP. (*C*) Current (Imem)/voltage (Vmem) relationship of the same cell as in *B* measured at the three ATP concentrations indicated. Current tracings on voltage ramp (0.03 Hz) stimulation were filtered at 1 kHz.

this concentration, depolarization was about half-maximal. Membrane potentials did not significantly change during this period of continued incubation, indicating that the bathing [ATP] was not decreased by hydrolysis of ATP and that the cells did not adapt to this [ATP] during this time.

In the patch-clamp experiments, cells were exposed to various [ATP] after measurement of the resting membrane potential. The membrane potentials measured for one cell at various doses of ATP are plotted in Fig. 4*B* as a function of [ATP_t]. The resting membrane potential of this cell was −79 mV. At 100 μM ATP_t, the membrane potential is modulated by the inward rectifying K^+ conductance (see below; Fig. 4*C*). In the whole-cell patch configuration, depolarization is complete at lower [ATP] than in microelectrode impalement studies, suggesting that cytoplasmic factors contribute to the shape of the dose–response curve in cells assessed by the latter technique. In 12 other whole-cell patch clamp experiments, similar results were obtained when the membrane potential was measured upon stepwise addition of ATP.

Fig. 4*C* shows a voltage clamp current/voltage relationship of the same cell as in Fig. 4*B*, measured at three different [ATP]. In the absence of ATP, the expression of the inward rectifying K^+ conductance is evident (13). At 100 μM ATP_t, the inward rectifier was partly counterbalanced by the ATP conductance, which caused the bistability in membrane potential (13) at low [ATP] (cf. Fig. 4*B*). At 350 μM ATP, the membrane conductance was dominated by the ATP conductance. These results show that the extent of ATP-induced depolarization depends on the expression of other conductances present in the membrane.

Recovery from Depolarization. In the microelectrode impalement experiment of Fig. 4*A*, after a final exposure to 3.2 mM ATP for 12 min, ATP was removed from the bath by replacing the medium. Membrane potentials were determined by measuring E_p as a function of time. The cells partly repolarized in the first minutes after removing ATP, and complete recovery took at least 90 min. This recovery period is much longer than in the whole-cell patch-clamp experiments in which intracellular ionic concentrations are clamped by the pipette solution (cf. Fig. 1). For cells studied by microelectrode impalement, this indicates that the ATP-induced pore allows the ionic constituents of the cells to exchange with the bathing solution as shown by Sung *et al.* (3). However, the cells remain capable of recovery from long-term (hours) exposure to [ATP] that causes incomplete depolarization (Fig. 4*A*) and from short-term (10 min; Fig. 4*A*) exposure to an [ATP] that causes complete depolarization.

Effects of ATP on ATPR B2 Cells and Mouse Peritoneal Macrophages. ATPR B2 is a J774.2-derived clone, selected as described, that is insensitive to ATP-induced membrane permeabilization (2, 4). ATPR B2 cells had a different peak potential distribution (median, −35 mV) compared with untreated J774.2 cells (median, −60 mV; Wilcoxon test, $P < 0.0006$), indicating that the ATP-resistant cells differed from the J774.2 cells in their resting membrane properties. When

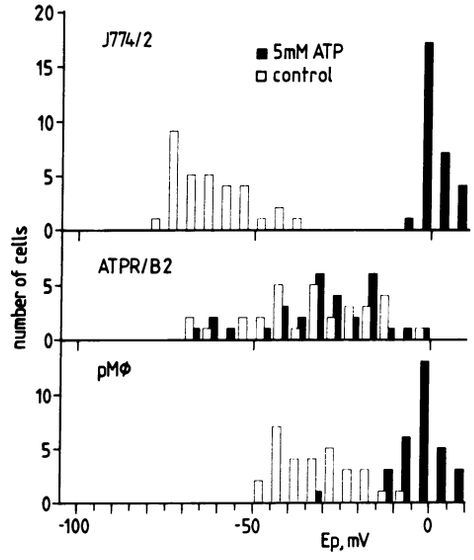

FIG. 5. Relative sensitivity to ATP of the macrophage cell lines J774.2 and ATPR B2 and of a 5-day culture of resident mouse peritoneal macrophages (pMϕ). Open bars, E_p upon microelectrode entry determined in ECS (control); solid bars, E_p after addition of 5 mM ATP_t (2.7 mM ATP^{4-}).

the ATP-resistant ATPR B2 cells were treated with 5 mM ATP_t, an [ATP] that fully depolarized J774.2 cells (Fig. 5), the ATPR B2 were not depolarized (Wilcoxon test, $P = 0.53$), consistent with the insensitivity of these cells to ATP-induced permeabilization (4). As expected, J774.2 cells were depolarized by this [ATP].

Mouse peritoneal macrophages had a resting membrane potential of about -35 mV. ATP treatment depolarized the membranes of these cells (Wilcoxon test, $P < 0.0006$). Thus, ATP-induced membrane depolarization occurs in primary macrophage explants as well as in transformed cell lines.

DISCUSSION

In the present study, we have shown with direct electrophysiological measurements that extracellular ATP^{4-} is a potent agonist for membrane depolarization in the J774.2 mouse macrophage-like cell line and in mouse peritoneal macrophages. The conductance involved is ion nonselective, activates rapidly (within 40 ms), has a whole-cell conductance of $\approx$10 nS, and half-maximally depolarizes intact cells at 13 μM ATP^{4-}.

In the whole-cell patch configuration the pipette solution replaces the intracellular solution (9), yet the rate of ATP-induced depolarization was still very high. From this we conclude that ATP-induced depolarizations are not mediated by a second messenger system but are a direct consequence of the ligation of receptors by ATP.

However, secondary effects of ATP receptors may affect the membrane potential. K^+ conductances can moderate the depolarizing effect of ATP. Three K^+ channels have been identified in mouse macrophages: a delayed outward rectifying K^+ conductance (14), an inward rectifying K^+ conductance, and a Ca^{2+}-activated K^+ conductance. The delayed outward rectifying K^+ conductance inactivates rapidly and cannot counterbalance a sustained depolarization.

By using both microelectrode impalement and whole-cell patch-clamp techniques, we have obtained evidence that both the inward rectifying K^+ conductance and the Ca^{2+}-activated K^+ conductance moderate ATP-induced depolarization. In our whole-cell patch-clamp measurements the intracellular $[Ca^{2+}]$ was fixed at 16 nM, thereby blocking the Ca^{2+}-activated K^+ conductance. Under these conditions, the inward rectifying K^+ conductance stabilized the membrane potential at $\leq$300 μM ATP (Fig. 4 *B* and *C*).

Considerably more ATP was required to depolarize J774.2 cells in the microelectrode impalement studies than in the whole-cell patch-clamp experiments. A likely explanation for this finding is the moderating effect of the Ca^{2+}-activated K^+ conductance of J774 cells (15, 16) on membrane potential in the intact cell measured by microelectrode impalement (17). Furthermore, Greenberg *et al.* (18) found that >100 μM ATP_t elevates the intracellular Ca^{2+} to the micromolar range in these cells. Although ATP dissipates transmembrane ionic gradients (3), the cells could maintain a membrane potential in the presence of up to 1.6 mM ATP_t, possibly due to the Ca^{2+}-activated K^+ conductance. Noninactivating K^+ channels in macrophages, therefore, may be important in preserving the membrane potential when low concentrations of extracellular ATP are applied. It is also possible that intracellular second messengers or other small soluble molecules, present in the cells studied by microelectrode impalement but not present in the whole-cell patch configuration, account for this finding.

We measured single-cell conductances of $\approx$10 nS by using the whole-cell patch configuration, and we estimated an upper limit of $\approx$20 pS for a single-channel conductance. If all channels were this size, a single cell would contain $\approx$500 channels. However, we have been unable to resolve single channels underlying the ATP-induced conductance. This is of interest in light of the finding of Cockcroft and Gomperts (1) that ATP permeabilizes mast cells to larger molecules at high [ATP] than at low [ATP]. One explanation could be that the ATP-induced conductance is not composed of measurable unitary conductances of a fixed size, but that the channels constitute a heterogeneous population of pores of variable conductance. The walls of such pores could be multimers of protein subunits, which aggregate under the influence of ATP. Such pore-forming multimers have been reported for several antibiotics (19).

Although ATP levels in blood are quite low, ischemic, injured, and dying cells can release ATP in large amounts. A number of cells release ATP, and platelet granules in particular contain a high concentration of this nucleotide. Therefore, macrophages might encounter extracellular ATP under certain circumstances. Macrophages secrete a vast number of substances. One suggestion for a function of the ATP^{4-}-induced pore in macrophages is that it might play a role in promoting secretion as in mast cells (20). Secretion also coincides with depolarization with an increase in intracellular $[Ca^{2+}]$ (21). Regardless of the physiologic function of ATP permeabilization, the present studies have demonstrated that this activity has specific biophysical properties and may constitute a ligand-dependent pore with distinctive characteristics and function.

We thank Ms. A. Annema for technical assistance, and Dr. A. A. Verveen for support and advice. This work was supported by a grant of the Netherlands Organization for Scientific Research (NWO) to H.P.B., a New York Lung Association Grant to T.H.S., Public Health Service Grant AI20516 to S.C.S., and the Cystic Fibrosis Research Development Program at Columbia University sponsored by the National Cystic Fibrosis Foundation.

1. Cockcroft, S. & Gomperts, B. D. (1979) *Nature (London)* **279,** 541–542.
2. Steinberg, T. H. & Silverstein, S. C. (1987) *J. Biol. Chem.* **262,** 3118–3122.
3. Sung, S.-S. J., Young, J. D.-E., Origlio, A. M., Heiple, J. M., Kaback, H. R. & Silverstein, S. C. (1985) *J. Biol. Chem.* **269,** 13442–13449.
4. Steinberg, T. H., Newman, A. S., Swanson, J. A. & Silverstein, S. C. (1987) *J. Biol. Chem.* **262,** 8884–8888.
5. Ralph, P. & Nakoinz, I. (1975) *Nature (London)* **257,** 393–394.
6. Van Furth, R. & Cohn, Z. A. (1968) *J. Exp. Med.* **128,** 415–435.
7. Fabiato, A. & Fabiato, F. (1979) *J. Physiol. (Paris)* **75,** 463–505.
8. Ince, C., Van Dissel, J. T. & Diesselhoff, M. M. C. (1985) *Pflügers Arch.* **403,** 240–244.
9. Hamill, O. P., Marty, A., Neher, E., Sakmann, B. & Sigworth, F. J. (1981) *Pflügers Arch.* **391,** 85–100.
10. Ince, C., Van Bavel, E., VanDuijn, B., Donkersloot, K., Coremans, A., Ypey, D. L. & Verveen, A. A. (1986) *Biophys. J.* **50,** 1203–1209.
11. Gomperts, B. D. (1983) *Nature (London)* **306,** 64–66.
12. Amano, F., Kitagawa, T. & Akamatsu, Y. (1984) *Biochim. Biophys. Acta* **803,** 163–173.
13. Gallin, E. K. & Livengood, D. R. (1981) *Am. J. Physiol.* **241,** C9–C17.
14. Ypey, D. L. & Clapham, D. (1984) *Proc. Natl. Acad. Sci. USA* **81,** 3083–3087.
15. Gallin, E. K. & Sheehy, P. A. (1985) *J. Physiol. (London)* **369,** 475–499.
16. Ince, C., Leijh, P. C. J., Meijer, J., Van Bavel, E. & Ypey, D. L. (1984) *J. Physiol. (London)* **352,** 625–635.
17. Barrett, J. N., Magleby, K. L. & Palotta, B. S. (1982) *J. Physiol. (London)* **331,** 211–230.
18. Greenberg, S., Di Virgilio, F., Steinberg, T. H. & Silverstein, S. C. (1988) *J. Biol. Chem.* **263,** 10337–10343.
19. De Kruijff, B. & Demel, R. A. (1974) *Biochim. Biophys. Acta* **339,** 57–70.
20. Bennett, J. P., Cockcroft, S. & Gomperts, B. D. (1981) *J. Physiol. (London)* **317,** 335–345.
21. Baker, P. F. & Knight, D. E. (1984) *Trends Neurosci.* **7,** 120–126.